Supporting Information

In-Situ Exfoliation of Copper-Based Metal−Organic Framework for Boosting Synergistic Photoactivation of Inert C(sp^3)−H Bonds and Oxygen

Huaqing Li,[‡a] Songtao Liu,[‡a] Guanfeng Ji,[a] Cheng He,[a] Yefei Wang,[a] Hui Gao,[a] Liang Zhao*[a] and Chunying Duan[b]

[a]State Key Laboratory of Fine Chemicals, Frontier Science Center for Smart Materials, Dalian University of Technology, Dalian 116024, P. R. China.

[b]State Key Laboratory of Coordination Chemistry, Nanjing University, Nanjing 210093, P. R. China.

[‡]These authors contributed equally to this work.

*Corresponding Author.

Email address: zhaol@dlut.edu.cn (L. Zhao)

Contents

1. Experimental Section.

Materials and Methods

All the chemicals and solvents were of reagent grade quality obtained from commercial sources and used without further purification. The ligand 9,10-dioxoanthracene-2,7-dicarboxylic acid (H_2**AQ**) was synthesized according to the methods in the reported literature and characterized by ^{1}H NMR.[1]

Powder X-ray diffraction (PXRD) measurements: The PXRD was obtained on a Rigaku Smart Lab XRD instrument with a sealed Cu tube (λ = 1.54178 Å).

Fourier transform infrared spectroscopy (FT-IR) measurements: The FT-IR was recorded from 400 to 4000 cm^{-1} on a ThermoFisher 6700 by using KBr pellets. All the spectra were collected neatly in the ambient atmosphere. The signals are given in transmittance (%) against wavenumbers (cm^{-1}).

Thermogravimetric analysis (TGA) measurements: The TGA analyses were performed on a TA Q500 instrument and recorded under N_2 followed by a ramp of 10 °C·min^{-1} up to 800 °C

Scanning electron microscopy (SEM) measurements: The SEM was performed on the JSM-7610F Plus field emission SEM under an accelerating voltage of 500 V. The samples were randomly dispersed on the surface of the flat aluminum sample holder for SEM measurements.

Energy-dispersive system (EDS) elemental mapping measurements: The EDX elemental mapping images were obtained on a JEOL JSM-7610F Plus Field Emission Scanning Electron Microscopy.

Transmission electron microscopy (TEM) measurements: TEM experiments were performed on a Tecnai G2 F30 S-Twin transmission electron microscope at an acceleration voltage of 300 kV.

Atomic force microscope (AFM) measurements: The AFM experiments were performed on an Environment Control Scanning Probe Microscope (JPK Nanowizard 4XP) and FastScan Bio (Bruker, USA) with the tapping mode in the air. The scan rate was 1 Hz, and the silicon tip was an OMCL-AC240TS-R3 (microcantilever, OLYMPUS) with a resonant frequency of 50 kHz and spring constant of 1.7 $N \cdot m^{-1}$ in air. Images were analyzed by JPKSPM Data Processing an open source software program developed for AFM images.

X-ray photoelectron spectroscopy (XPS) measurements: The XPS signals were collected on a Thermo ESCALAB Xi+ spectrometer.

Sorption studies: N_2 adsorption/desorption was determined with autosorb iQ physical adsorption instrument at 77 K. The samples were degassed for 6 hours at 120 °C, under the pressure below 1 Torr.

The solid-state ultraviolet-visible (UV-Vis) absorption spectra: Liquid UV-Vis spectra were collected on a PERSEE T9CS spectrometer. Solid UV-Vis spectra were recorded on Hitachi U-4100 UV-Vis-NIR spectrophotometer with the standard reference of $BaSO_4$ powder.

The gas chromatography-mass spectrometry (GC-MS) measurements: The GC-MS analyses were performed on Agilent Technologies 7890B GC system and Agilent 5977B MSD system.

The Time of flight mass spectrometry (TOF MS) measurements: The TOF MS analyses were performed on Agilent Technologies G6224A GC system.

Electron paramagnetic resonance (EPR) measurements: The EPR spectrums were recorded on BRUKER E500 equipped with a liquid N_2 system.

Nuclear magnetic resonance measurements: The ^1H NMR spectra were recorded on the Vaian DLG400 with internal standard TMS at δ 0.0 ppm.

Electrochemical Experiments

Photocurrent measurements were conducted with a ZAHNER ENNIUM electrochemical workstation in a standard three-electrode system with the photocatalyst-coated FTO as the working electrode, Pt plate as the counter electrode in an aqueous solution of KCl at a scan rate of 100 mV/s, and an Ag/AgCl as a reference electrode. A 420 nm LED was used as the light source. The 2.0 mg of catalyst was added into 250 μL of CH_3CH_2OH and 20 μL of Nafion mixed solution. Then a 100 μL suspension was dropped on the surface of an FTO glass and dried at room temperature for photocurrent measurements, and the signals were recorded under 10 s chopped light. Electrochemical impedance spectroscopy (EIS) and Mott-Schottky plots were performed with a 30 μL suspension on the working electrode with a bias potential of −0.5 V.

Dye Uptake Experiment Preparation of Cu−AQ-NS.

The exfoliated crystals nanosheets Cu−**AQ**-NS were soaked in a methanol solution of methylene blue dye. After shook at room temperature, the resulting dark brown crystals were washed with methanol several times until the filter liquor became colorless to remove the dye adsorbed on the surface of the crystals. Further, the saturated absorption crystals were dissociated by hydrochloric acid, and the solution was diluted to 10 mL.

Preparation of Crystals with NH_4Cl.

The crystals were soaked in an acetonitrile solution of NH_4Cl. After shook at room temperature for 24 hours, the resulting crystals were washed with acetonitrile several times to remove the NH_4Cl adsorbed on the surface of the crystals. The crystals with NH_4Cl were dried in vacuum overnight.

Confocal Laser Scanning Microscopy

The fresh crystals of Cu−**AQ**-NS were soaked in a saturated methanol solution of 2',7'-dichlorofluorescein and handled in the same way with the experiments of dye uptake. The brightfield and confocal images of the processed samples were scanned at λ_{em} = 510−610 nm, exited by 488 nm through a 405/488 nm filter.

Chlorine Radical Trapping Experiments

The chlorine radical trapping experiment was carried out in an 8.0 mL quartz tube in which a mixture of styrene (0.4 mmol), DBAD (0.4 mmol), Cu−**AQ**-NS (6.0 μmol), NH_4Cl (0.03 mmol) and CH_3CN (3.0 mL) was added for 12 hours. After completion, the residues were analyzed by TOF MS.

Carbon Radical Trapping Experiments.

The carbon radical trapping experiment was carried out in an 8.0 mL quartz tube in which a mixture of the catalyst Cu−**AQ**-NS (6.0 μmol), cyclohexane (0.4 mmol), NH_4Cl (0.03 mmol) and CH_3CN (3.0 mL) was added. After 30 minutes of continuous stirring container irradiated with 420 nm LED at room temperature in argon, 2,2,6,6-tetramethyl-1-piperidinyloxy (0.4 mmol) was added as a radical scavenger for 12 hours. After completion, the residues were analyzed by TOF MS.

Molecular Oxygen Activation Measurements

The 3,3',5,5'-tetramethylbenzidine (TMB) oxidation experiments were measured

according to previous reports.[2] 2 mL of CH_3CN or CH_3OH suspension containing the catalyst (1 mg/mL), NH_4Cl (1 mg/mL) and 6 mg of TMB (3 mg/mL CH_3CN or CH_3OH solution) were mixed in the cuvette. A 420 nm LED equipment was used as the light source. TMB oxidation experiments were evaluated by UV-Vis measurements at different time intervals.

Reactive Oxygen Species Trapping Experiment.

The $O_2^{\bullet-}$ and $^1O_2$ generated by Cu−**AQ**-NS have been detected by EPR in the presence of DMPO and TEMP, respectively.[3] Typically, 30 μL DMPO or TEMP in 1 mL CH_3CN was mixed with 0.5 mL suspension of Cu−**AQ**-NS (2 mg), NH_4Cl (2 mg) and CH_3CN (2 mL). The formed mixed solution is drawn with a capillary tube and placed into an EPR tube. EPR measurements were carried out during the 420 nm LED light irradiation under air condition.

2. Characterizations of Metal-Organic Framework.

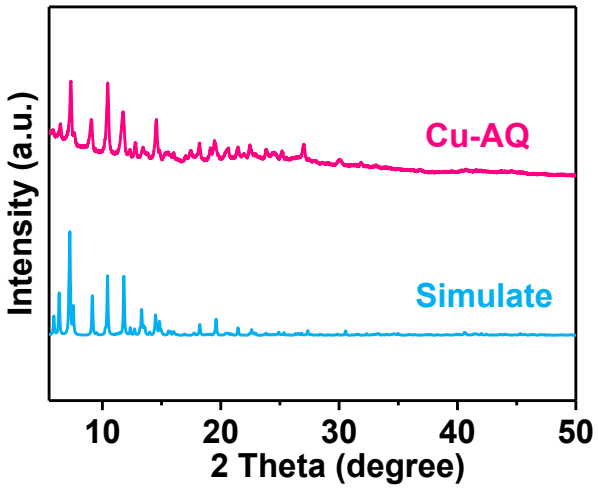

Figure S1. PXRD pattern of Cu−**AQ**.

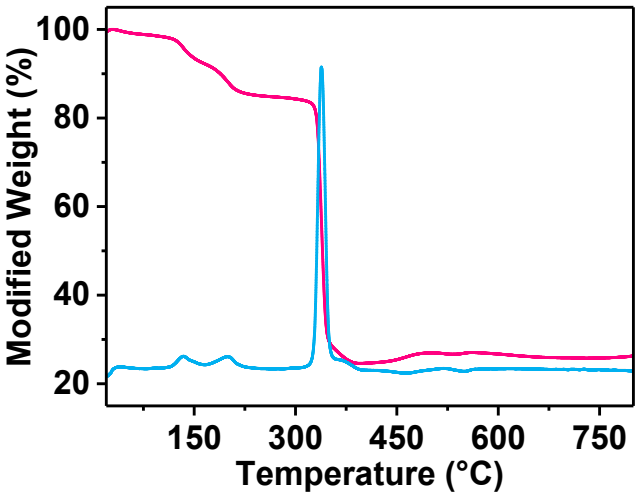

Figure S2. Thermogravimetric analyses (TGA) of the as-synthesized Cu−**AQ**. The data was collected under N_2 followed by a ramp of 10 °C·min^{-1} up to 800 °C.

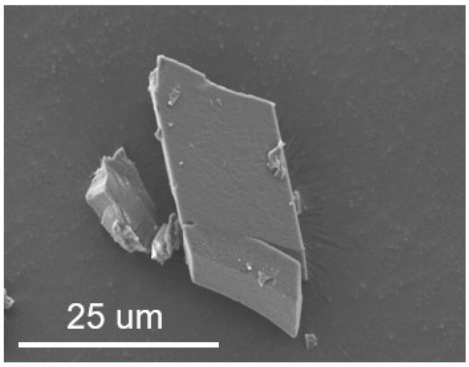

Figure S3. The SEM image of the Cu−**AQ**.

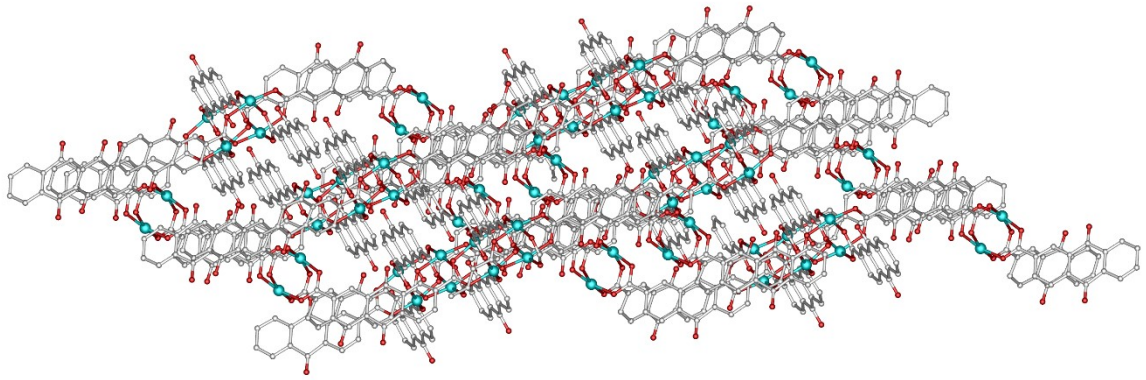

Figure S4. The 3D layered Cu−**AQ** viewed along the (1-11) direction.

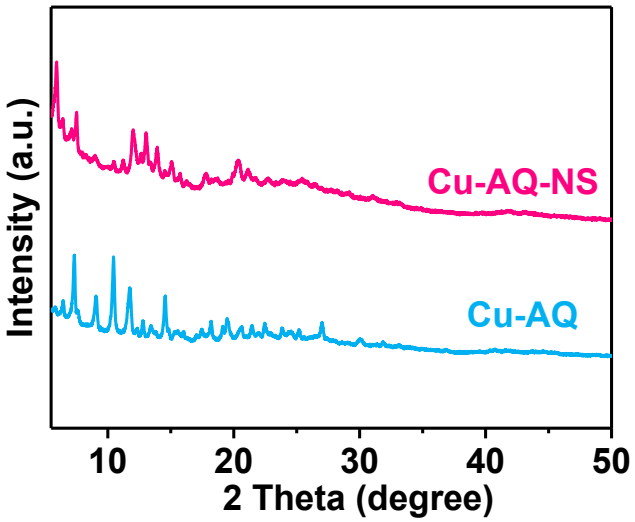

Figure S5. PXRD pattern of Cu−**AQ** and Cu−**AQ**-NS.

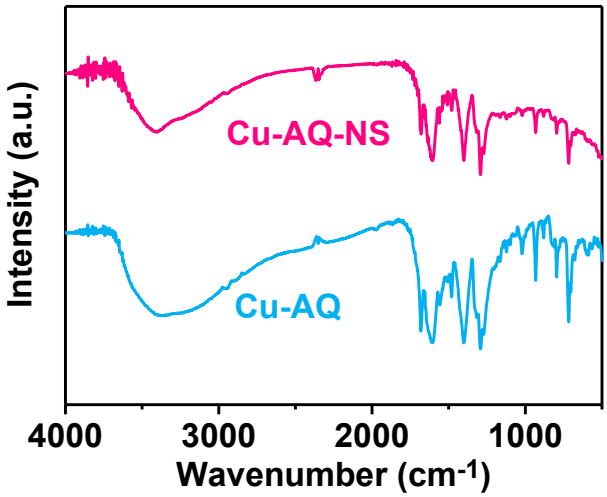

Figure S6. IR spectra of Cu−**AQ** and Cu−**AQ**-NS.

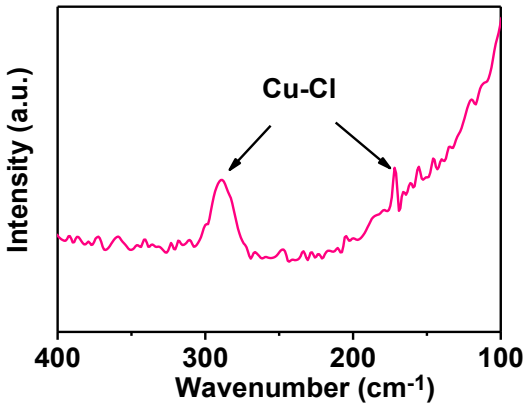

Figure S7. The Raman spectrum of Cu−**AQ**-NS with NH_4Cl.

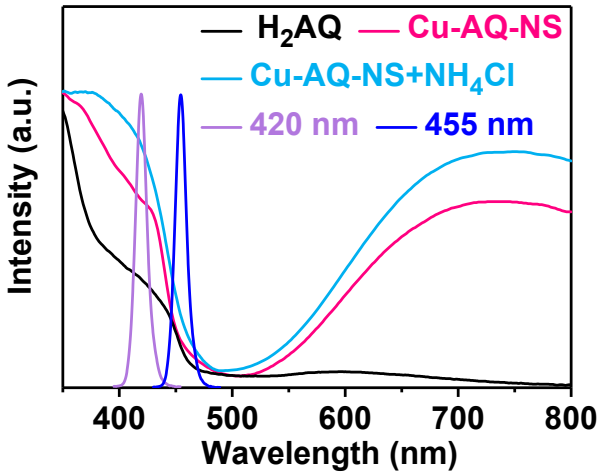

Figure S8. UV-Vis absorption spectrum of H_2**AQ** (black), Cu−**AQ**-NS (red) and Cu−**AQ**-NS adding NH_4Cl (blue).

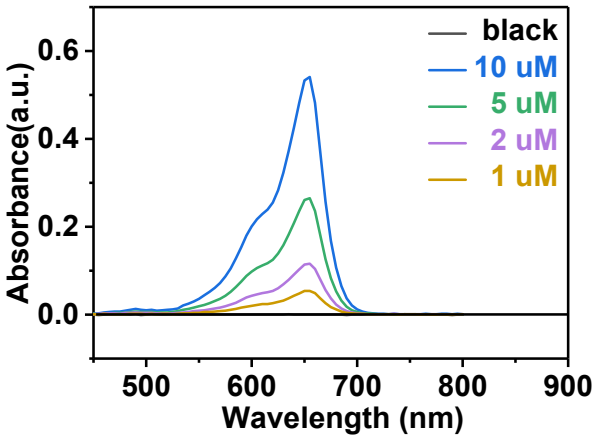

Figure S9. UV-Vis spectrum of different concentrations of methylene blue dye.

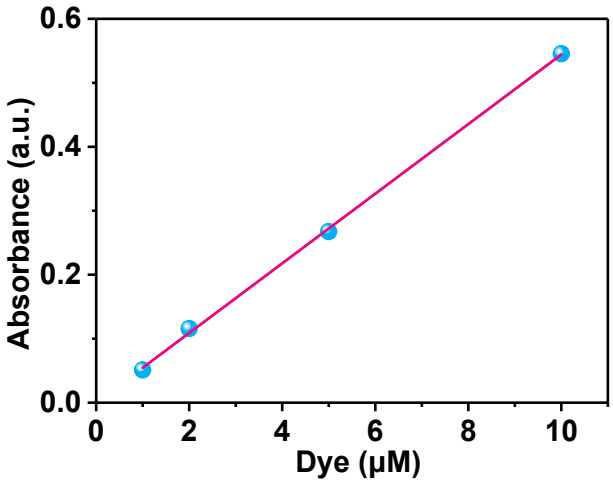

Figure S10. The standard linear relationship between the absorbance and the concentration of methylene blue dye with a correlation coefficient of 0.99971 by the corresponding absorbance changes at 665 nm. Calculation equation: y = 0.00018 + 0.0544x, Where, y is the absorbance intensity of methylene blue dye solution, x is the molar concentration of the methylene blue dye.

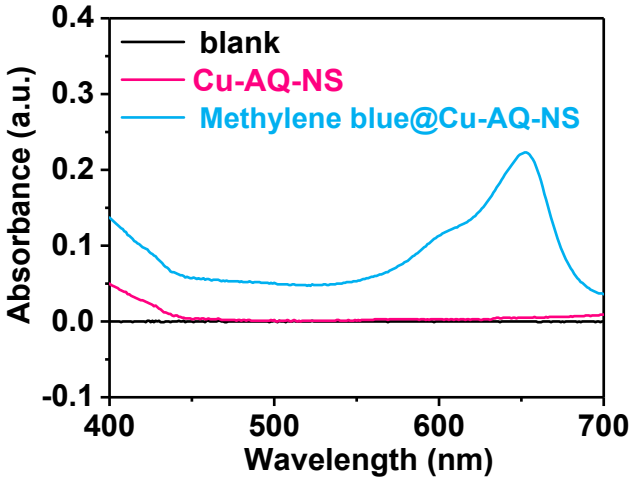

Figure S11. The UV-Vis spectrum of Cu−**AQ**-NS (5 mg) before (red line) and after (blue line) adsorption of methylene blue. The quantum uptake of dye is calculated at 26.1 wt% of the Cu−**AQ**-NS weight according to the standard linear relationship between the absorbance and the concentration of dye.

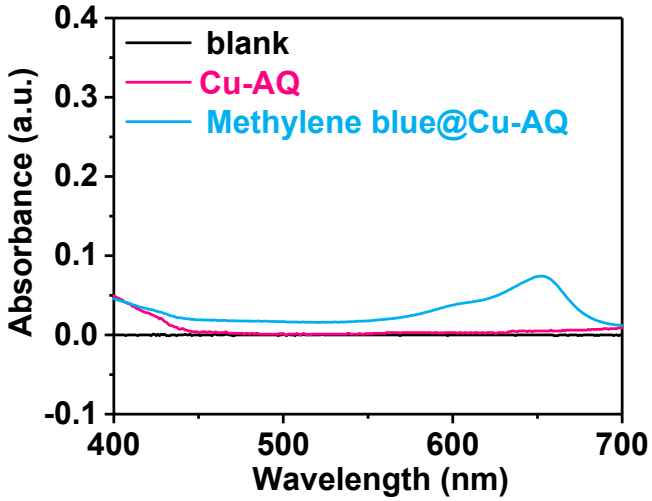

Figure S12. The UV-Vis spectrum of Cu−**AQ** (5 mg) before (red line) and after (blue line) adsorption of methylene blue. The quantum uptake of dye is calculated at 8.8 wt% of the Cu−**AQ**-NS weight according to the standard linear relationship between the absorbance and the concentration of dye.

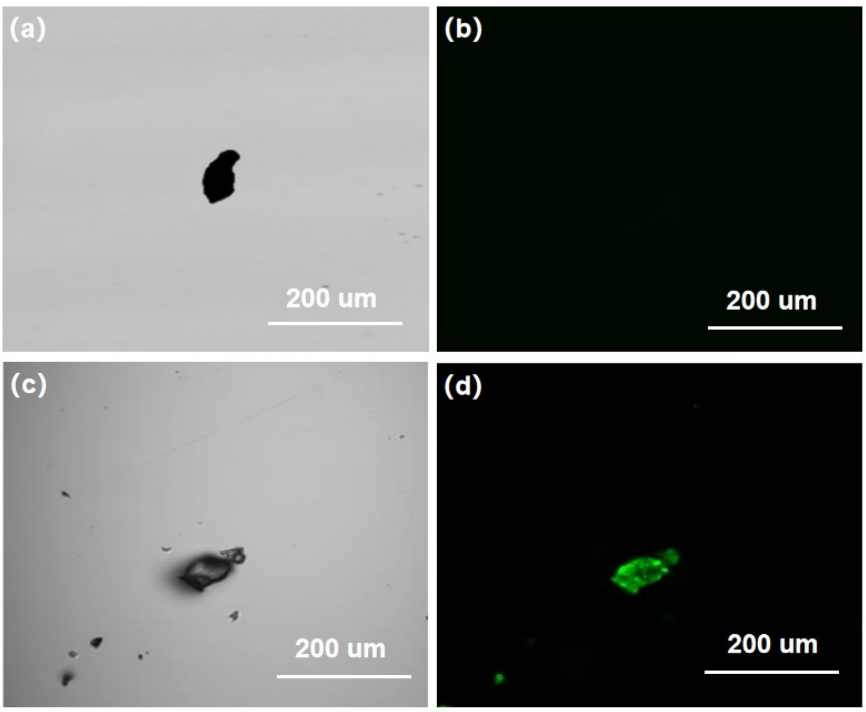

Figure S13. Confocal images of Cu−**AQ**-NS empty (a and b) and soaked (c and d) 2',7'-dichlorofluorescein dye. Bright-field images (a and c) and dark-field images (b and d) were detected at λ_{em}: 510–610 nm, λ_{ex}: 488 nm through a 405/488 nm filter.

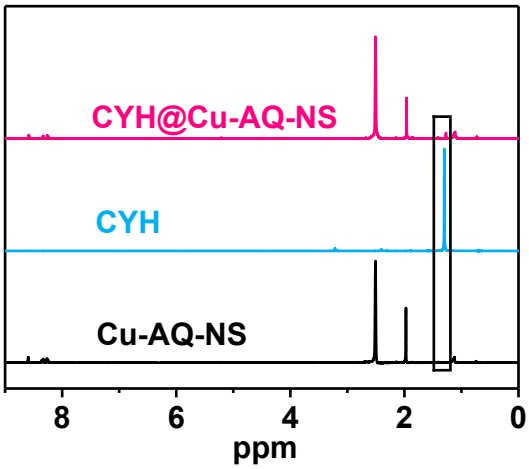

Figure S14. ^{1}H NMR of Cu−**AQ**-NS before (black line) and after (blue line) absorption of the cyclohexane in DMSO-d_6/D_2SO_4. ^{1}H NMR of cyclohexane (red line) in DMSO-d_6/D_2SO_4.

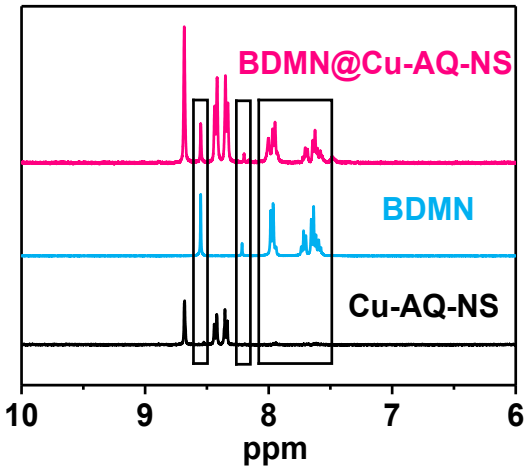

Figure S15. ^{1}H NMR of Cu−**AQ**-NS before (black line) and after (blue line) absorption of the benzylidenemalononitrile in DMSO-d_6/D_2SO_4. ^{1}H NMR of benzylidenemalononitrile (red line) in DMSO-d_6/D_2SO_4.

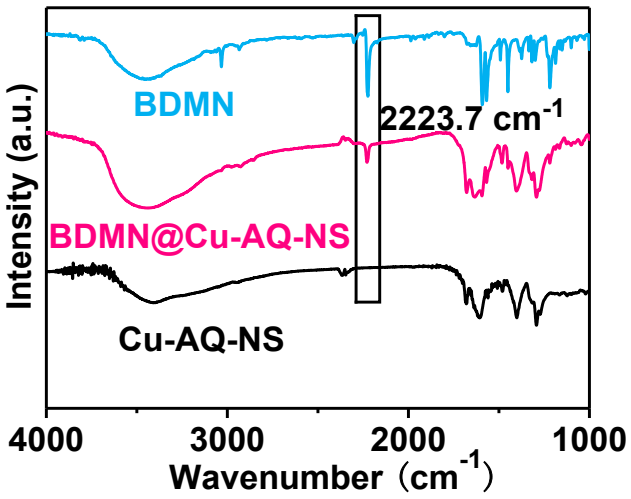

Figure S16. IR spectrum of Cu−**AQ**-NS before (black line) and after (red line) impregnated in acetonitrile solution containing benzylidenemalononitrile (0.1 mM), benzylidenemalononitrile (blue line). The peak at 2223.7 cm^{-1} on the IR spectrum belonged to the characteristic peak of the benzylidenemalononitrile.

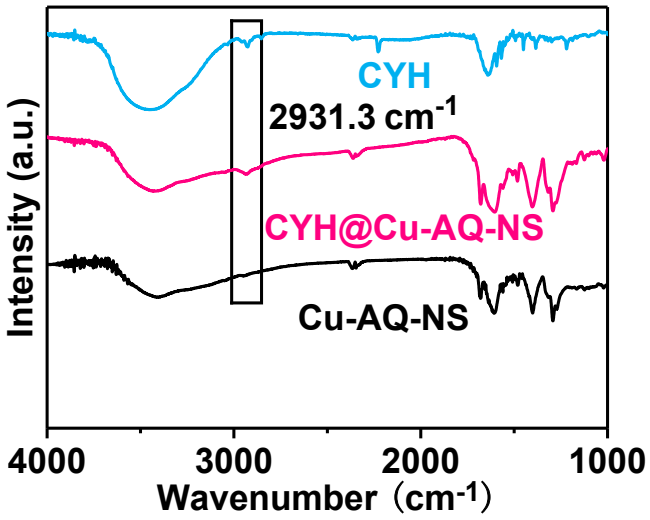

Figure S17. IR spectrum of Cu−**AQ**-NS before (black line) and after (red line) impregnated in acetonitrile solution containing cyclohexane (0.1 mM), cyclohexane (blue line). The peak at 2931.3 cm^{-1} on IR spectrum belonged to the characteristic peak of the cyclohexane.

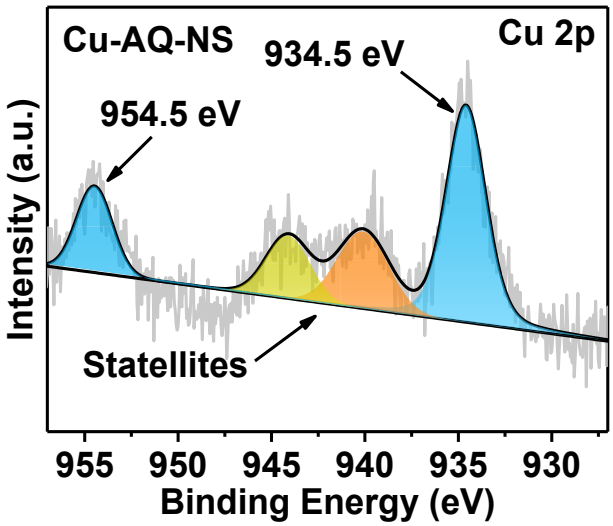

Figure S18. The magnified Cu 2p XPS spectra of Cu−**AQ**-NS.

Table S1. Assignment of the Cu 2p components from Figure S18.

Ionic state	Spin-orbit doublet	BE (eV)	FWHM (eV)
Cu^{II}	$2p_{3/2}$	934.5	3.2
	$2p_{1/2}$	954.5	3.2

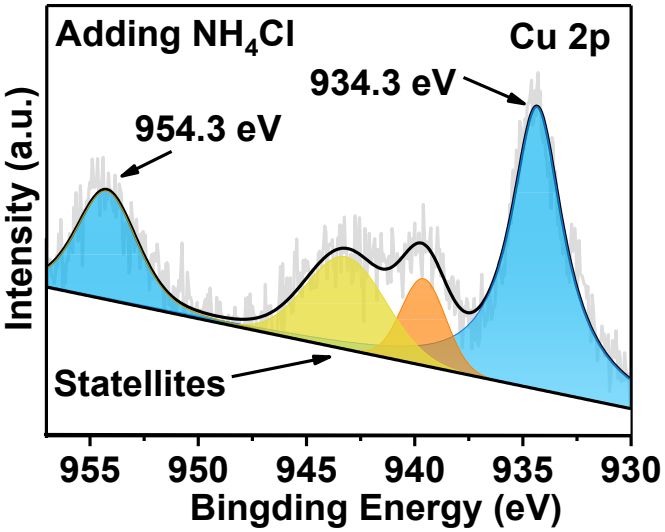

Figure S19. The magnified Cu 2p XPS spectra of Cu−**AQ**-NS adding NH_4Cl.

Table S2. Assignment of the Cu 2p components from Figure S19.

Ionic state	Spin-orbit doublet	BE(eV)	FWHM(eV)
Cu^{II}	$2p_{3/2}$	934.3	2.9
	$2p_{1/2}$	954.3	3.2

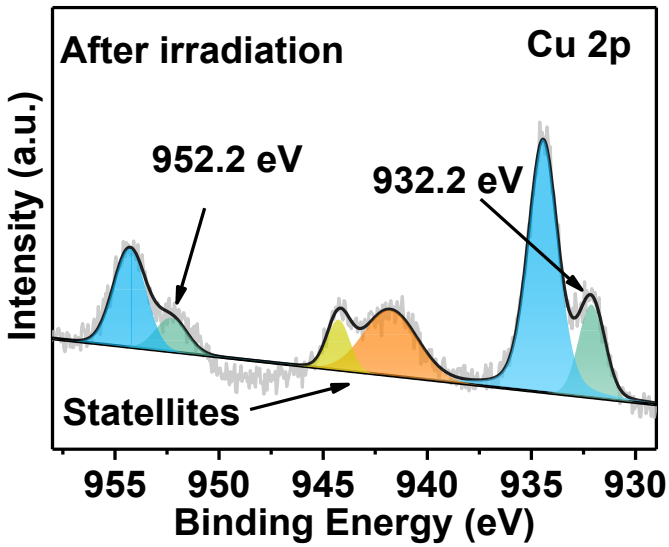

Figure S20. The magnified Cu 2p XPS spectra of Cu−**AQ**-NS adding NH_4Cl after irradiation.

Table S3. Assignment of the Cu 2p components from Figure S20.

Ionic state	Spin-orbit doublet	BE(eV)	FWHM(eV)
Cu^{II}	$2p_{3/2}$	934.5	2.1
	$2p_{1/2}$	954.5	2.4
Cu^{I}	$2p_{3/2}$	932.2	1.3
	$2p_{1/2}$	952.2	1.6

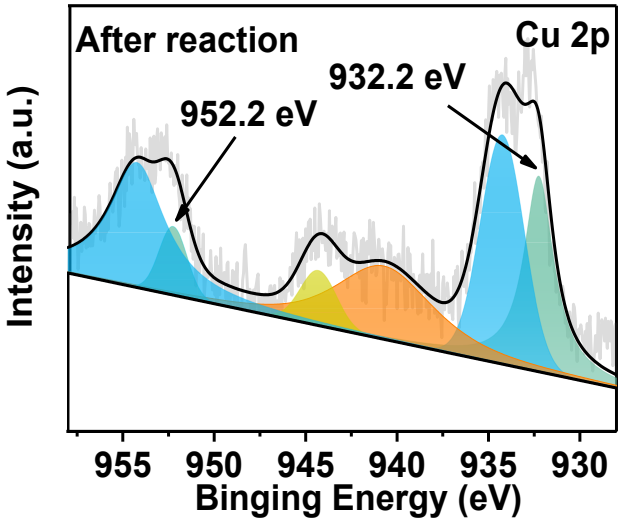

Figure S21. The magnified Cu 2p XPS spectra of Cu−**AQ**-NS with NH_4Cl after the cyclohexane arylation.

Table S4. Assignment of the Cu 2p components from Figure S22.

Ionic state	Spin-orbit doublet	BE(eV)	FWHM(eV)
Cu^{II}	$2p_{3/2}$	934.3	2.8
	$2p_{1/2}$	954.3	3.6
Cu^{I}	$2p_{3/2}$	932.2	1.9
	$2p_{1/2}$	952.2	1.8

3. Catalysis Details

General Procedure for Photocatalytic Arylation of Inert C(sp^3)−H Bonds.

The photocatalytic arylation of inert C(sp^3)−H bonds was performed in a sealed quartz flask containing catalysts (6.0 μmol), benzylidenemalononitrile (0.1 mmol), substrates (0.5 mL) and NH_4Cl (0.03 mmol) in CH_3CN (3 mL) in Ar atmosphere under 420 nm LED at 30 °C within 8 hours. The yields were determined by ^1H NMR spectroscopy using 0.1mmol 1,3,5-trimethoxybenzene as an internal standard.

General Procedures for Photocatalytic Oxidation of Inert C(sp^3)−H bonds.

The photocatalyzed oxidation of inert C(sp^3)−H bonds was performed in a sealed quartz flask containing catalysts (6.0 μmol), substrates (0.1 mmol) and NH_4Cl (0.03 mmol) in CH_3CN (3 mL) in O_2 atmosphere under 420 nm LED at 30 °C within 24 hours. The yields were determined by GC analysis with 0.1 mmol 1,3,5-trimethoxybenzene as an internal standard.

Cycle Catalysis Experiment.

After the photocatalytic reaction, the mixture was centrifuged at 8000 rpm for 5 min, and the precipitate was washed with CH_3CN until no product was detected in the eluent. The recovered solid was reused for the next runs directly.

Table S5. Photocatalytic oxidation of cyclohexane under different conditions.

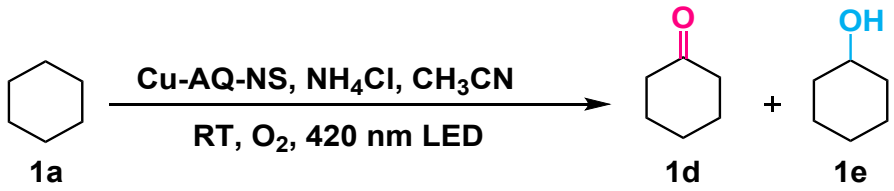

Entry	Variation from the standard condition	Yield (%)		Selectivity (%)
		1d	1e	
1	None	61	1	98
2	455 nm LED instead of 420 nm LED	13	6	68
3	No light	N.R.	N.R.	–
4	No NH_4Cl	Trace	Trace	–
5	No Cu–**AQ**-NS	N.R.	N.R.	–

Standard condition: Cu–**AQ**-NS (6.0 μmol), cyclohexane (0.1 mmol) and NH_4Cl (0.03 mmol) in CH_3CN (3 mL) in O_2 atmosphere under 420 nm LED at 30 °C within 24 hours. Yields were determined by GC analysis with 0.1 mmol 1,3,5-trimethoxybenzene as an internal standard.

Table S6. Photocatalytic oxidation of α-terpinene.

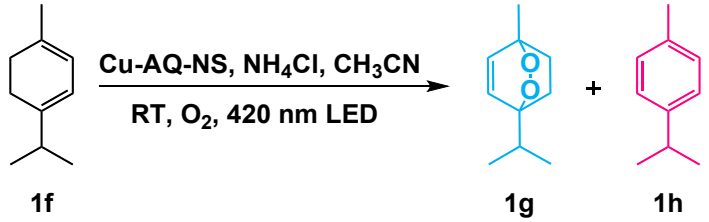

1f **1g** **1h**

Entry	Catalyst	Selectivity (%)	
		1g	1h
1	H_2**AQ**	90	10
2	Cu−**AQ**-NS	25	75

Standard condition: α-terpinene (0.1 mmol), catalyst (6.0 μmol), NH_4Cl (0.03 mmol) in acetonitrile (5 mL) under irradiation with a 420 nm LED in an oxygen atmosphere within 6 hours. The selectivity was determined by GC analysis with 0.1 mmol 1,3,5-trimethoxybenzene as an internal standard.

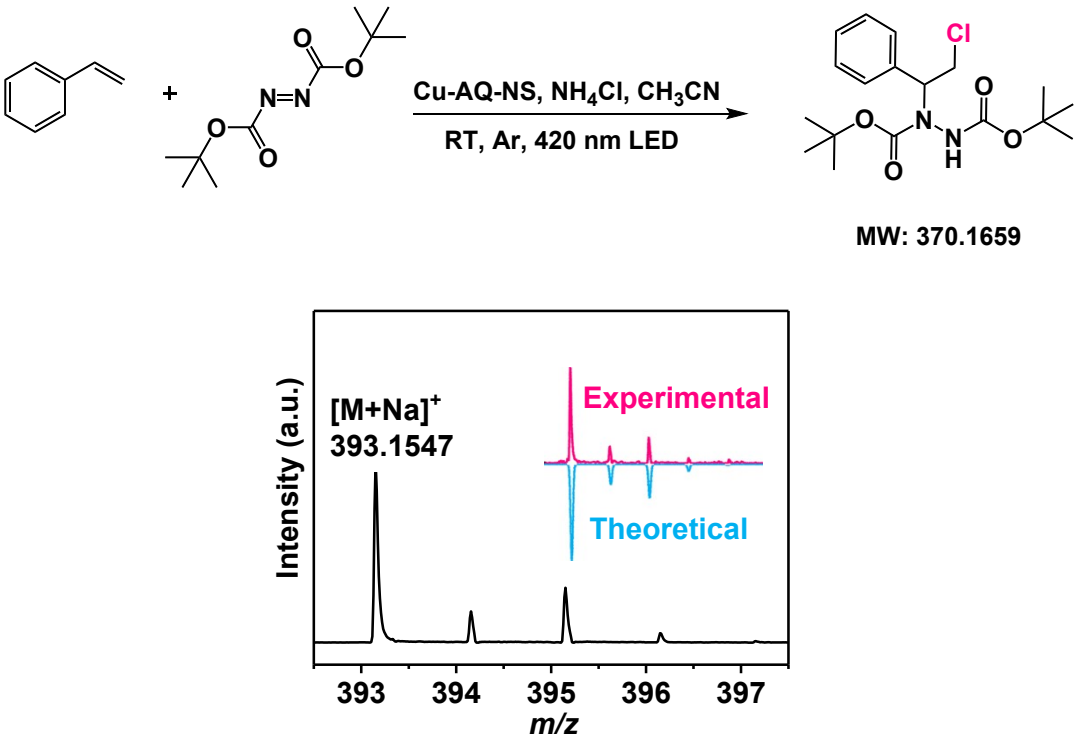

Figure S22. Chlorine radical trapping experiments with styrene, DBAD, Cu−**AQ**-NS, and NH_4Cl; The ESI-MS spectrum shows the chlorine radical adduct with DBAD and styrene. ESI-MS: calcd for $C_{18}H_{27}N_2O_4Cl$: 370.1659. Found for $[M+Na]^+$ 393.1547.

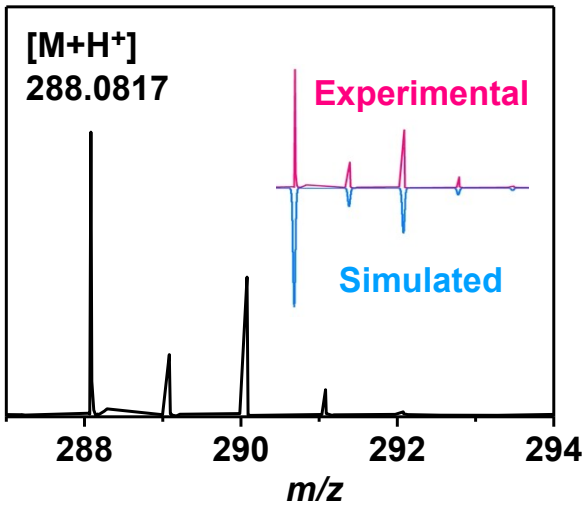

Figure S23. Carbon radical trapping experiments with Ts protected bis allyl amines under standard condition. ESI-MS: calcd for $C_{13}H_{18}ClNO_2S$: 287.0747; Found for $[M+H]^+$ 288.0817.

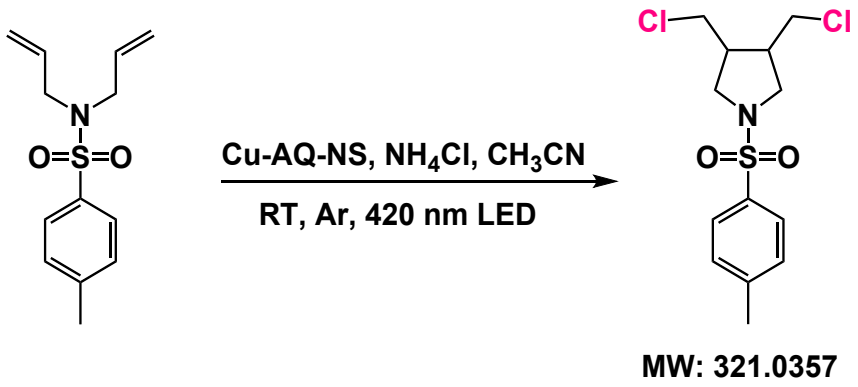

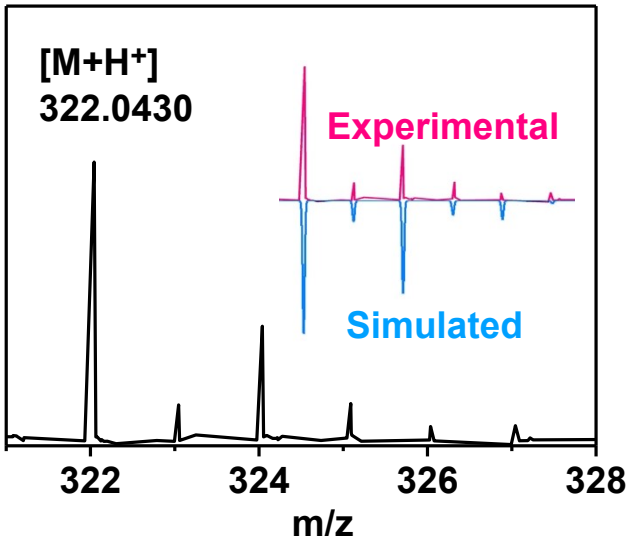

Figure S24. Carbon radical trapping experiments with Ts protected bis allyl amines under standard condition. ESI-MS: calcd for $C_{13}H_{17}Cl_2NO_2S$: 321.0357; Found for $[M+H]^+$ 322.0430.

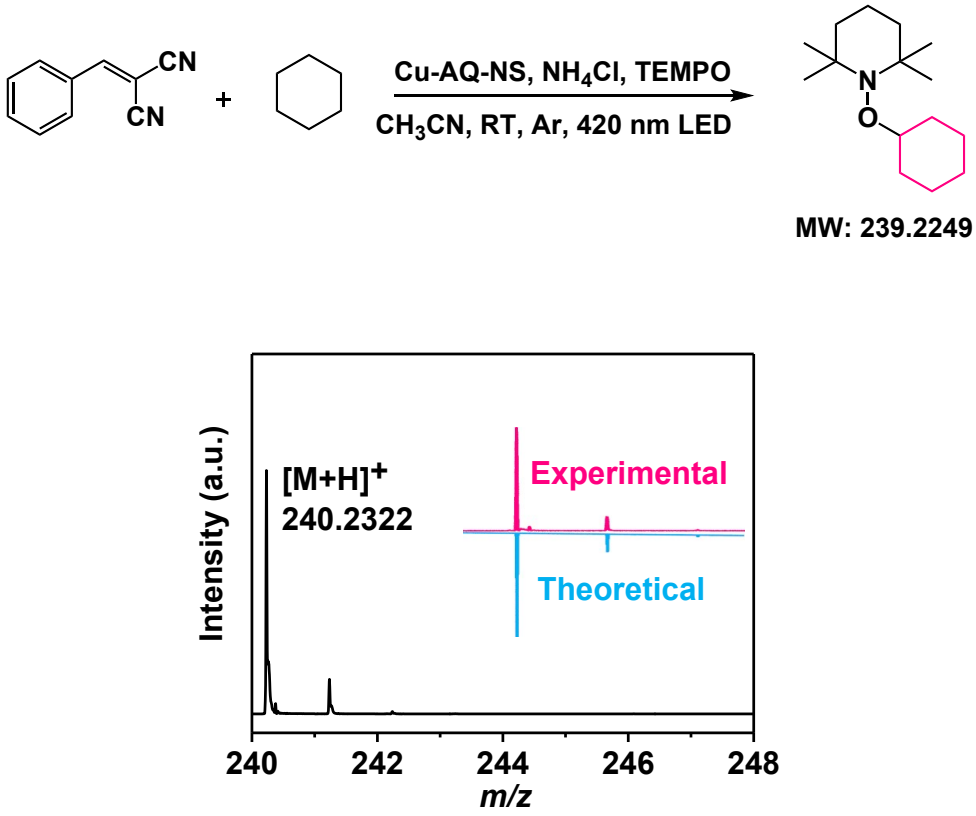

Figure S25. Carbon radical trapping experiments with TEMPO under standard condition. ESI-MS: calcd for $C_{15}H_{29}NO$: 239.2249; Found for $[M+H]^+$ 240.2322.

Scheme S1. Deuterium Labeling Experiments. The mixture kinetic isotope effect (KIE) experiment for the arylation of cyclohexane and cyclohexane-d_{12} under the standard condition.

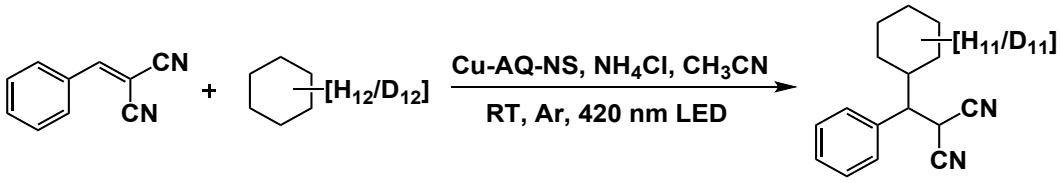

Standard condition: Benzylidenemalononitrile (0.1 mmol), cyclohexane (1.0 mmol), cyclohexane-d_{12} (1.0 mmol), NH_4Cl (0.03 mmol) and Cu−**AQ**-NS (6.0 μmol) in acetonitrile (3.0 mL) under irradiation with a 420 nm LED in Ar atmosphere within 12 h. The yields were determined by ^1H NMR spectroscopy using 0.1mmol 1,3,5-trimethoxybenzene as an internal standard (k_H/k_D = 4.12).

Scheme S2. Deuterium Labeling Experiments. The parallel kinetic isotope effect (KIE) experiment for the arylation of cyclohexane and cyclohexane-d_{12} under the standard condition.

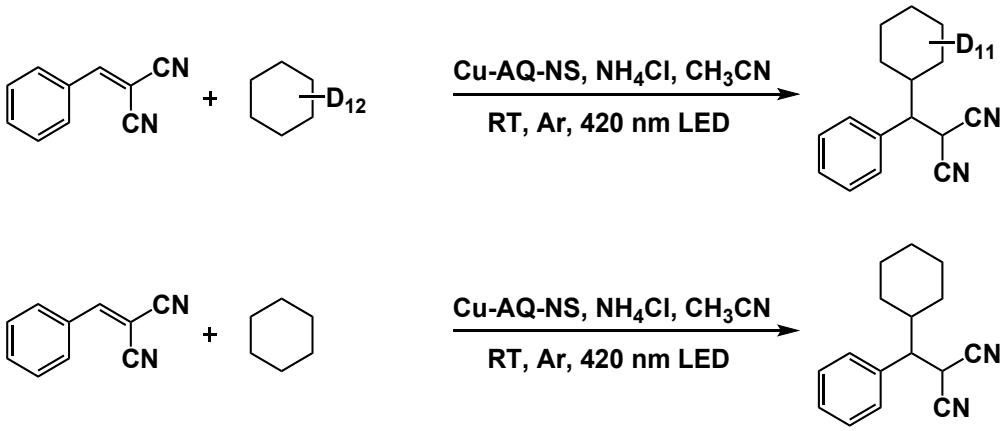

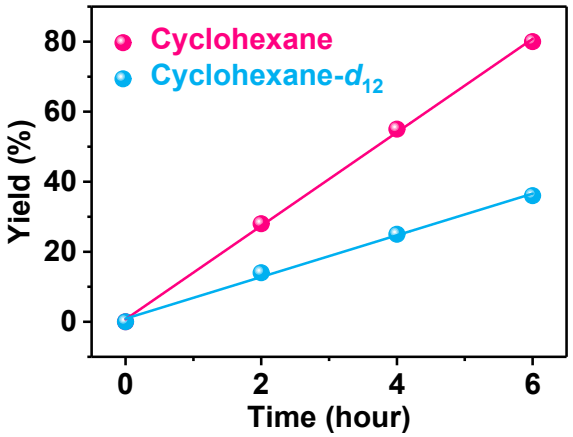

Standard condition: Benzylidenemalononitrile (0.1 mmol), cyclohexane-d_{12} (1.0 mmol), NH_4Cl (0.03 mmol) and Cu−**AQ**-NS (6.0 μmol) in acetonitrile (3.0 mL) under irradiation with a 420 nm LED in Ar atmosphere. The yields were determined by ^1H NMR spectroscopy using 0.1mmol 1,3,5-trimethoxybenzene as an internal standard (k_H/k_D = 2.21).

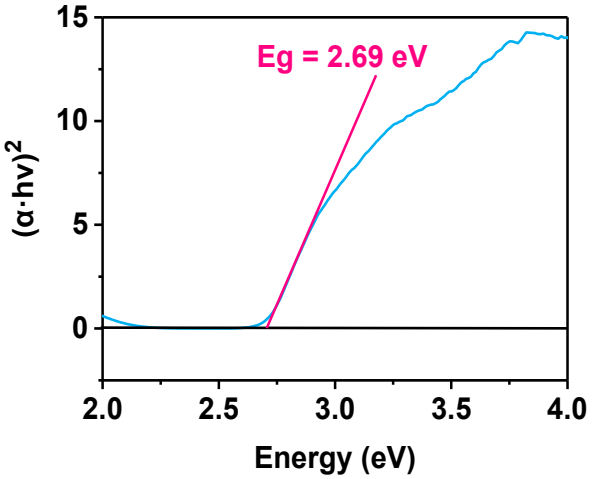

Figure S26. The Tauc plot of Cu−**AQ**-NS.

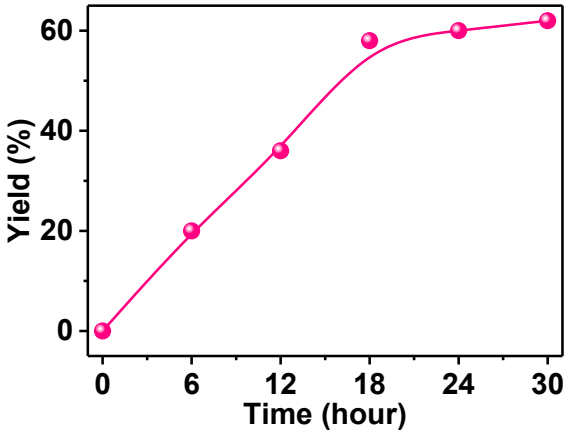

Figure S27. Yields of target product as a function of the time with cyclohexane (0.1 mmol), NH_4Cl (0.03 mmol) and Cu−**AQ**-NS (6.0 μmol) in acetonitrile (3 mL) under irradiation with a 420 nm LED in an oxygen atmosphere.

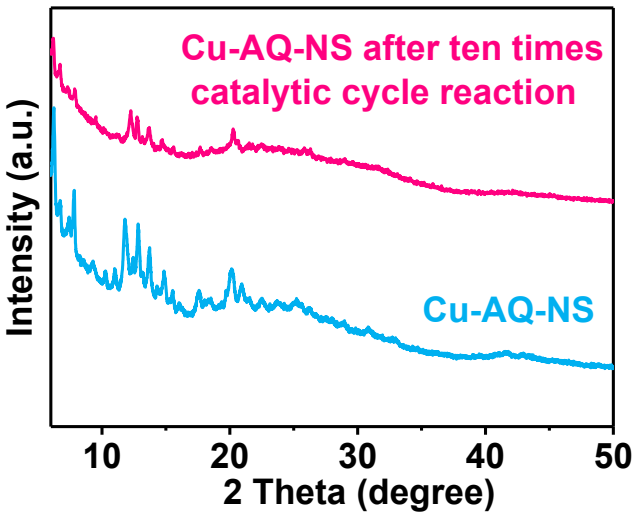

Figure S28. PXRD pattern of Cu−**AQ**-NS and Cu−**AQ**-NS after ten times catalytic cycle reaction.

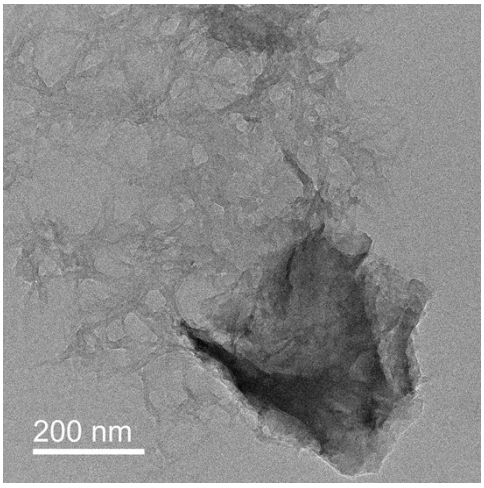

Figure S29. The TEM image of the Cu−**AQ**-NS after ten times catalytic cycle reaction.

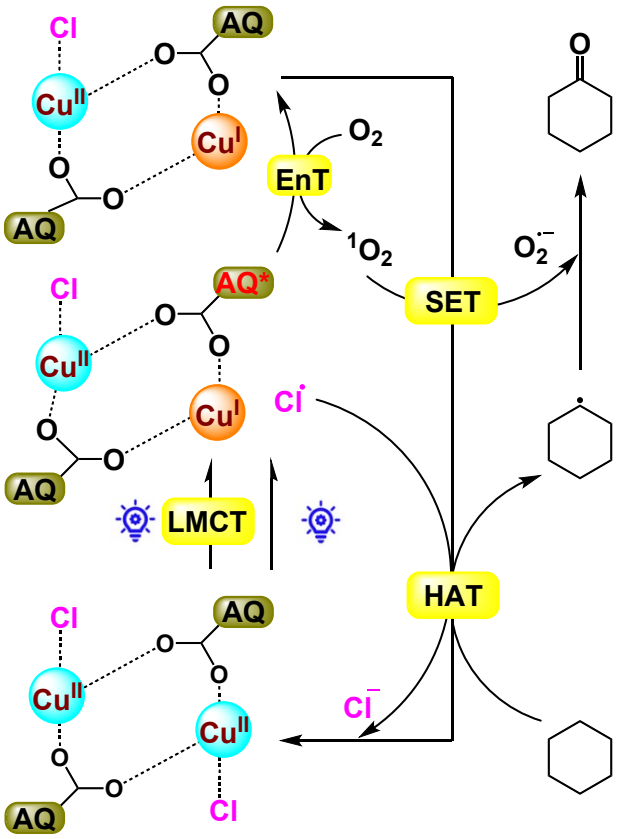

Figure S30. Proposed photocatalytic mechanism of cyclohexane C(sp^3)−H oxidation.

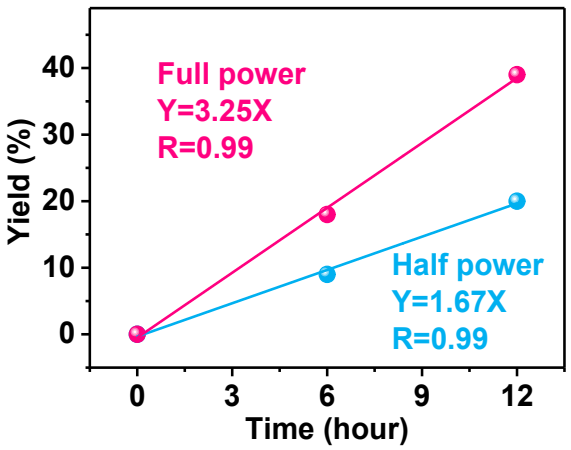

Figure S31. Two photooxygenation reactions yields of cyclohexane as a function of the time under the standard condition with a 420 nm LED irradiation of full power (k_F) and half power (k_H), respectively (k_F/k_H = 1.95).

4. Copies of ^{1}H NMR Spectrum

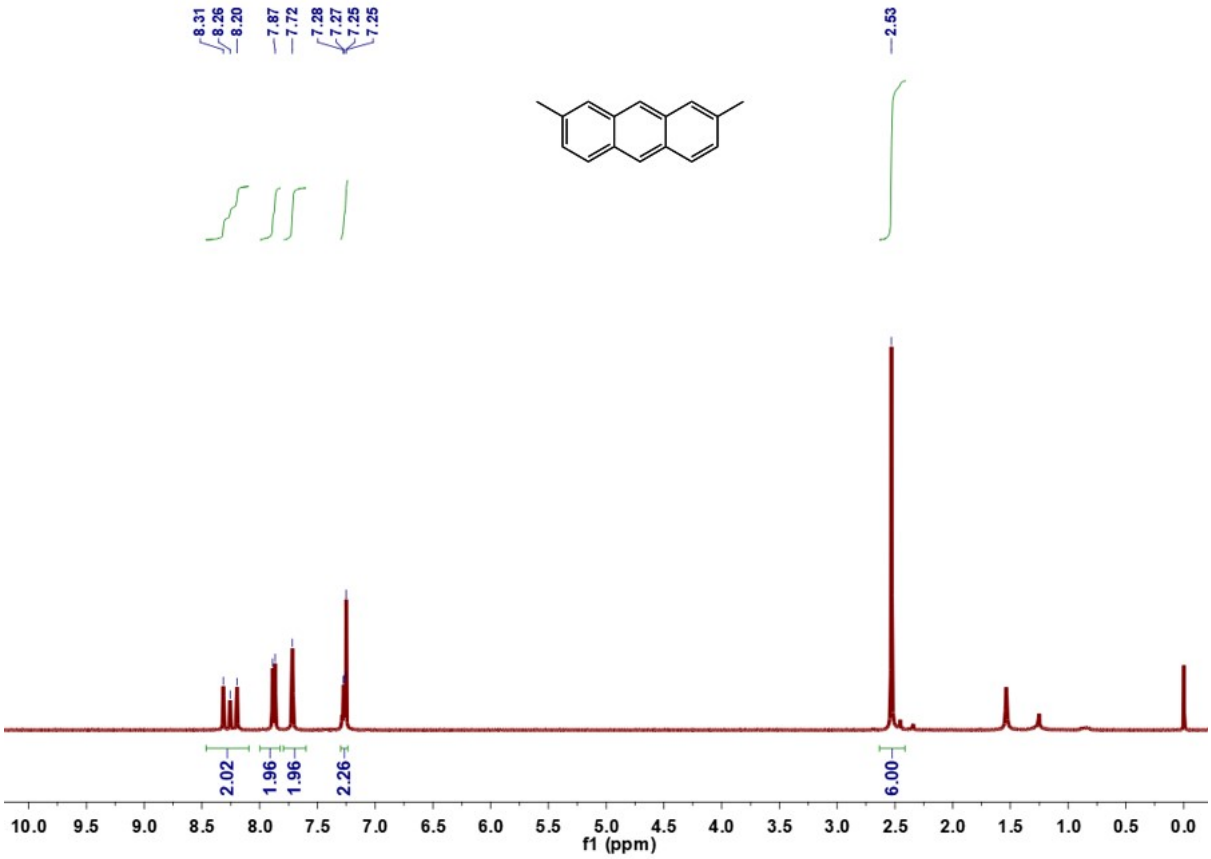

Figure S32. ^{1}H NMR spectra of the 2,7-dimethylanthracene. ^{1}H NMR (600 MHz, $CDCl_3$, ppm): δ 8.32−8.20 (m, 2H), 7.88 (d, J = 8.6 Hz, 2H), 7.72 (s, 2H), 7.28−7.25 (m, 2H), 2.53 (s, 6H).

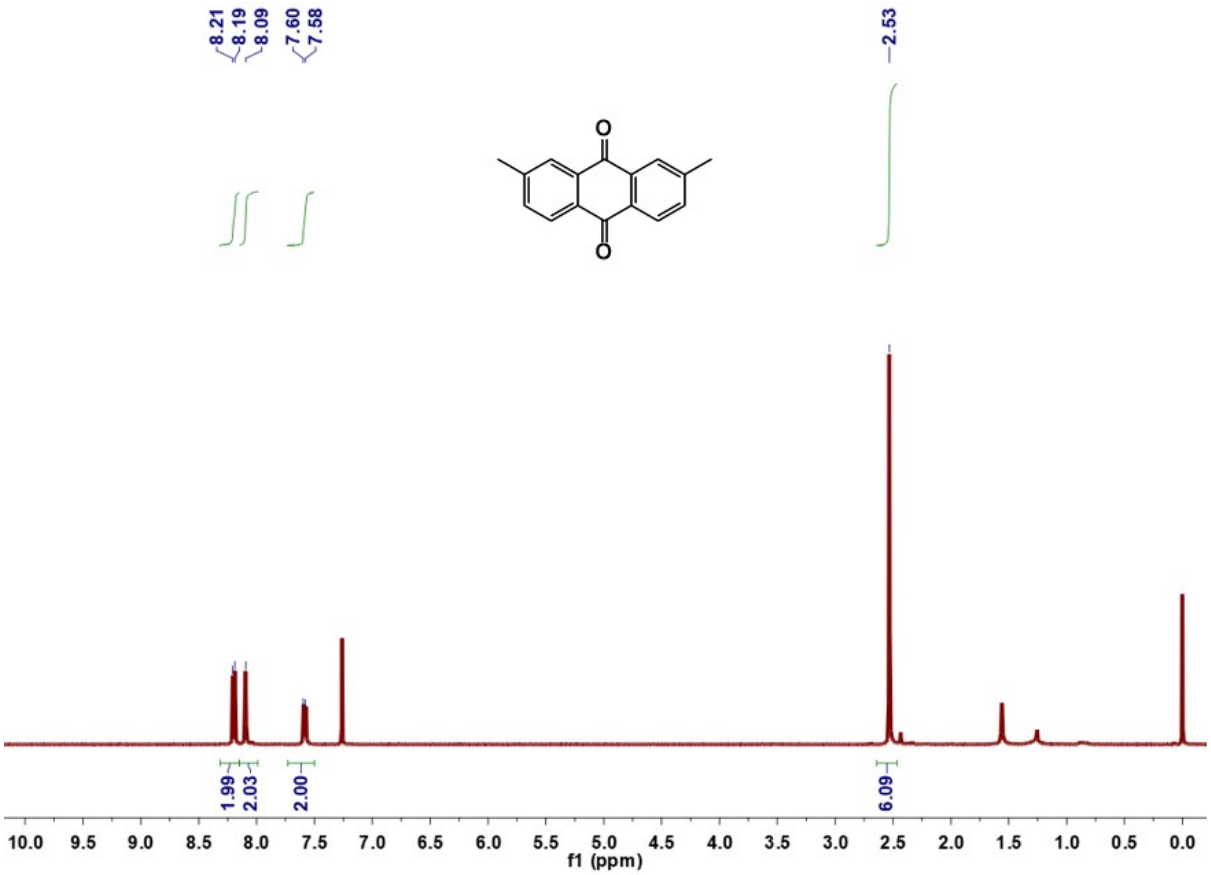

Figure S33. ^{1}H NMR spectra of the 2,7-dimethylanthraquinone. ^{1}H NMR (600 MHz, $CDCl_3$, ppm): δ 8.20 (d, J = 12.0 Hz, 2H), 8.09 (s, 2H), 7.59 (d, J = 12.0 Hz, 2H), 2.53 (s, 6H).

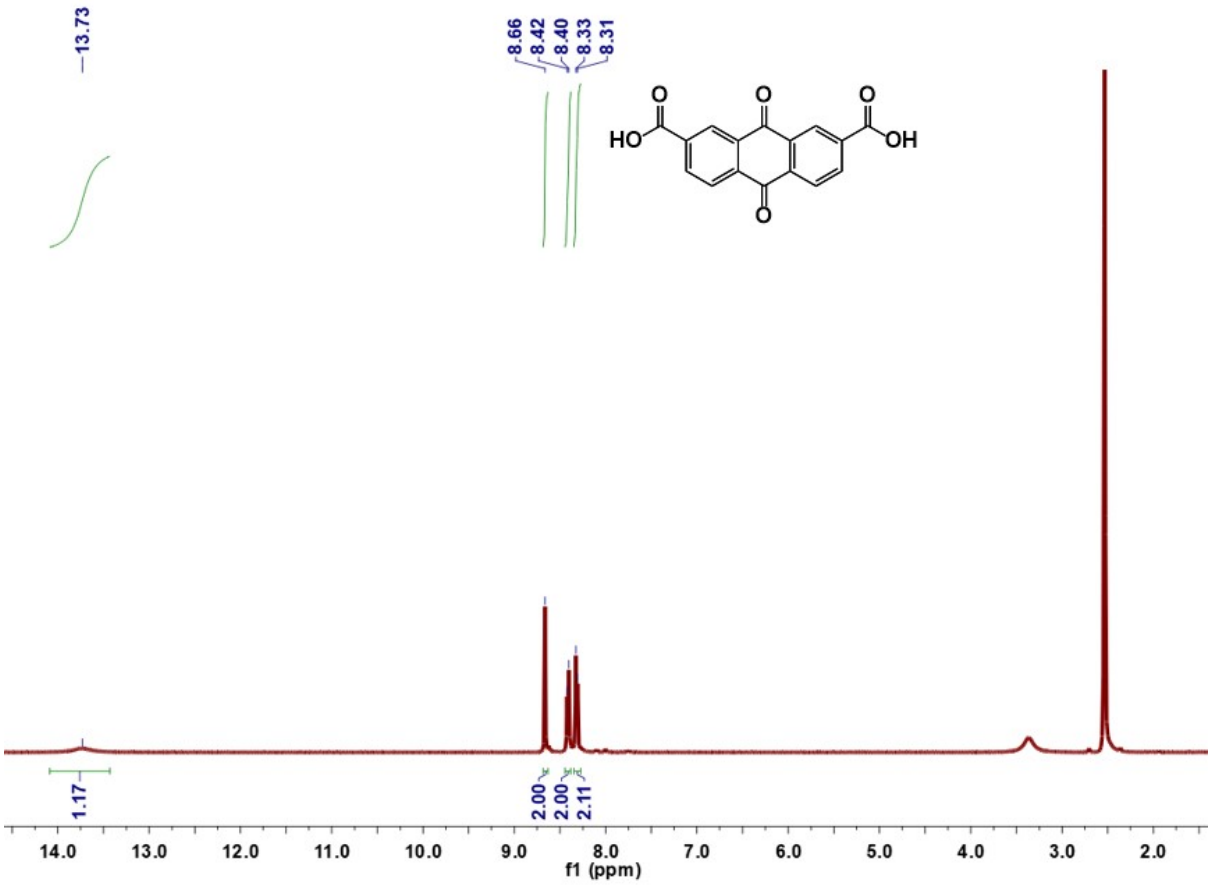

Figure S34. ^{1}H NMR spectra of the H_2**AQ**. ^{1}H NMR (600 MHz, DMSO-d_6, ppm): δ 13.73 (s, 1H), 8.66 (s, 2H), 8.40 (d, J = 12.0 Hz, 2H), 8.32 (d, J = 12.0 Hz, 2H).

It has been reported that the characteristic peaks of 1,3,5-trimethoxybenzene are 3.75 and 6.08 ppm.[3] The integration number of the peak at 6.08 ppm represents the equivalent of the internal standard relative to the substrate.

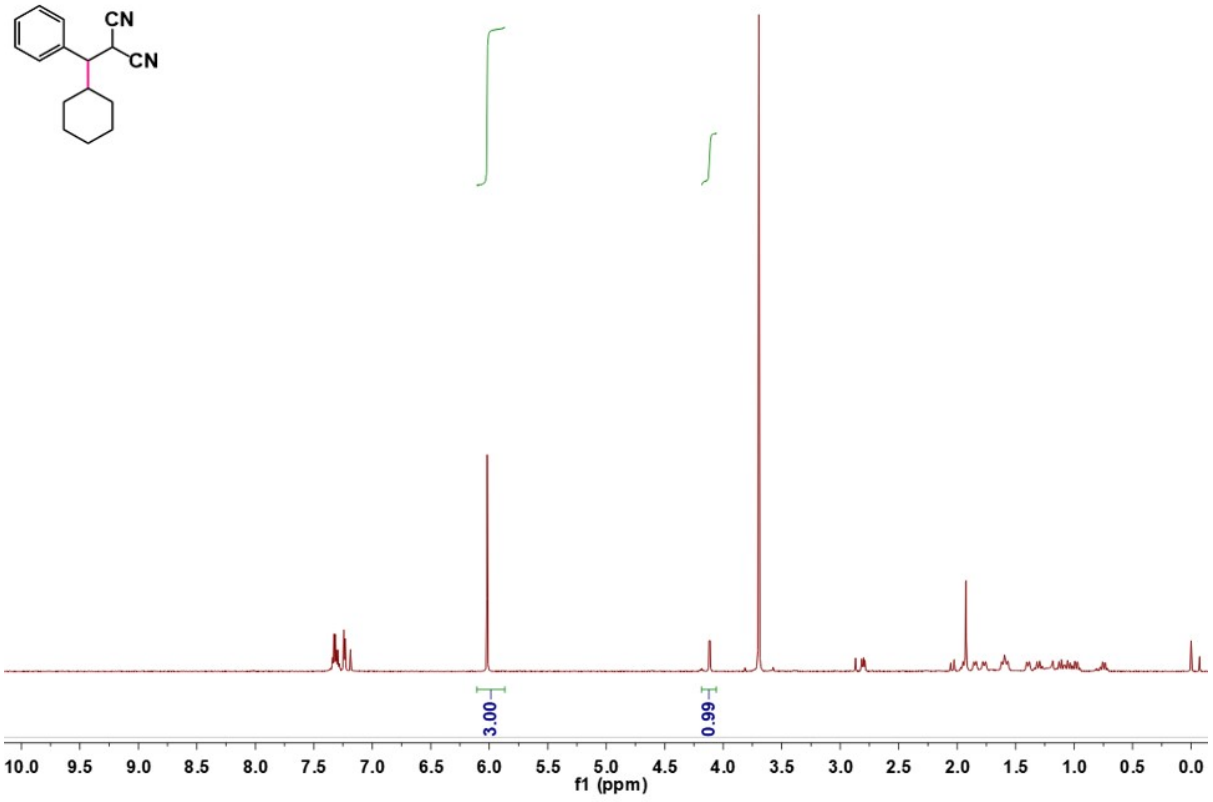

Figure S35. Crude ^{1}H NMR Spectrum for **1c**.

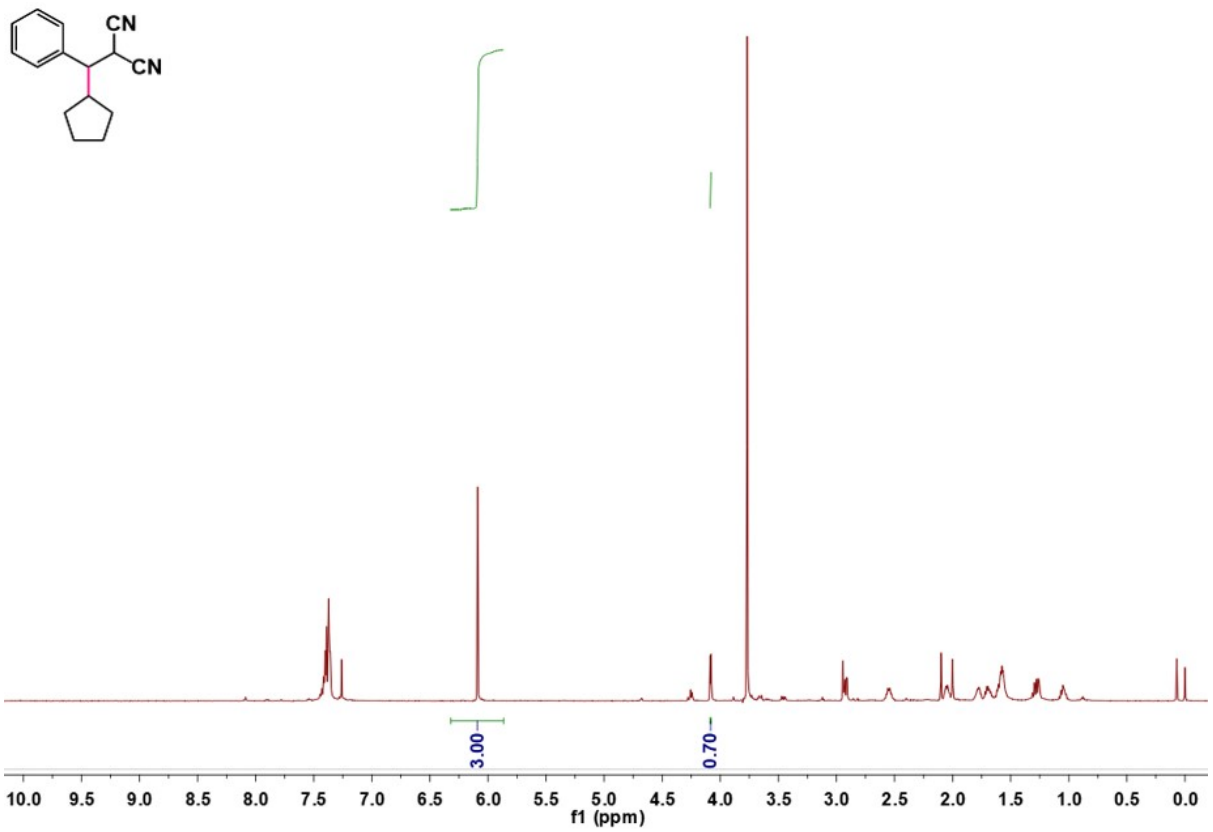

Figure S36. Crude ^{1}H NMR Spectrum for **2c**.

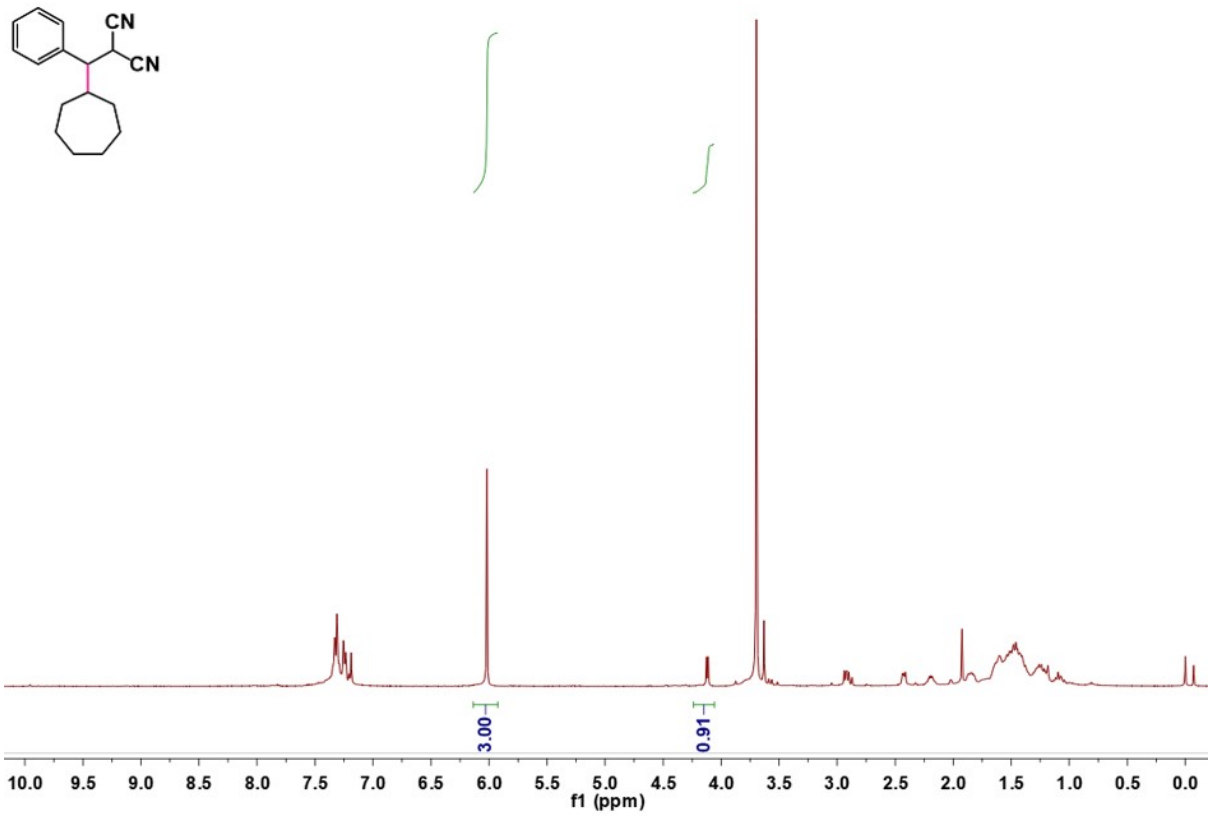

Figure S37. Crude ^{1}H NMR Spectrum for **3c**.

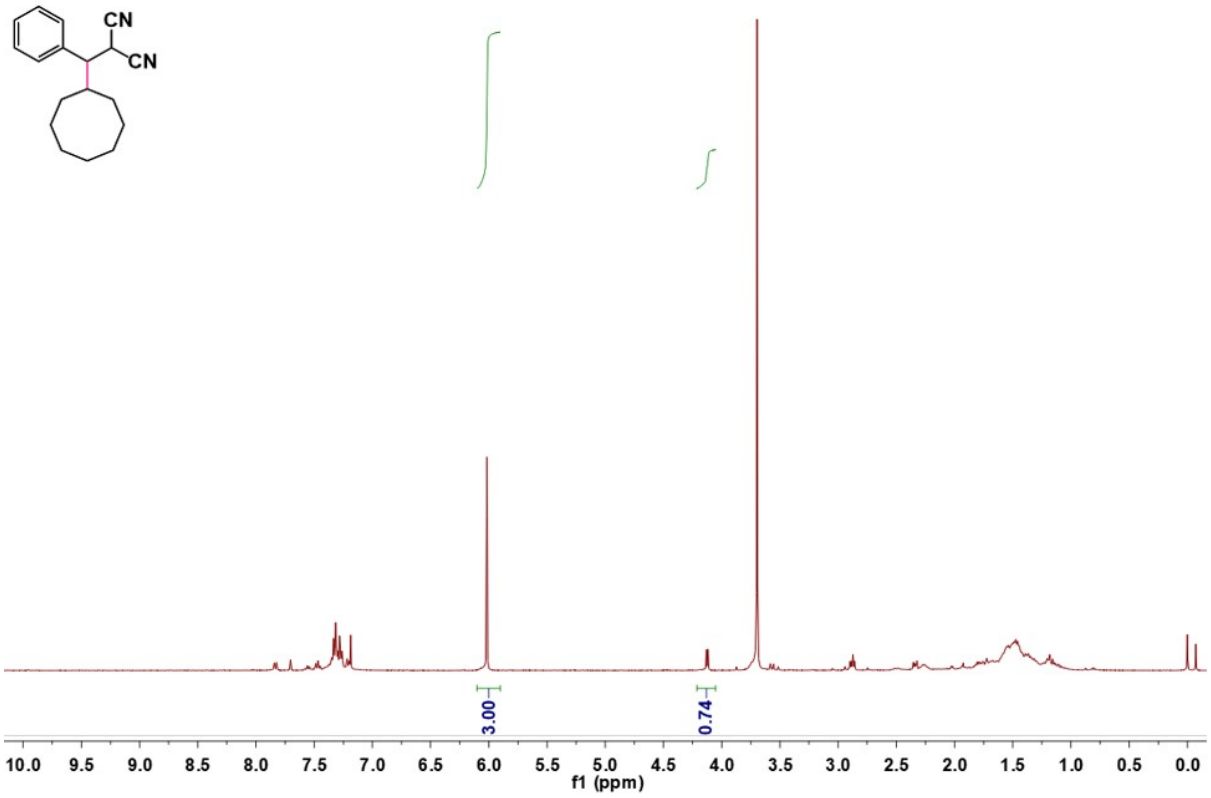

Figure S38. Crude ^{1}H NMR Spectrum for **4c**.

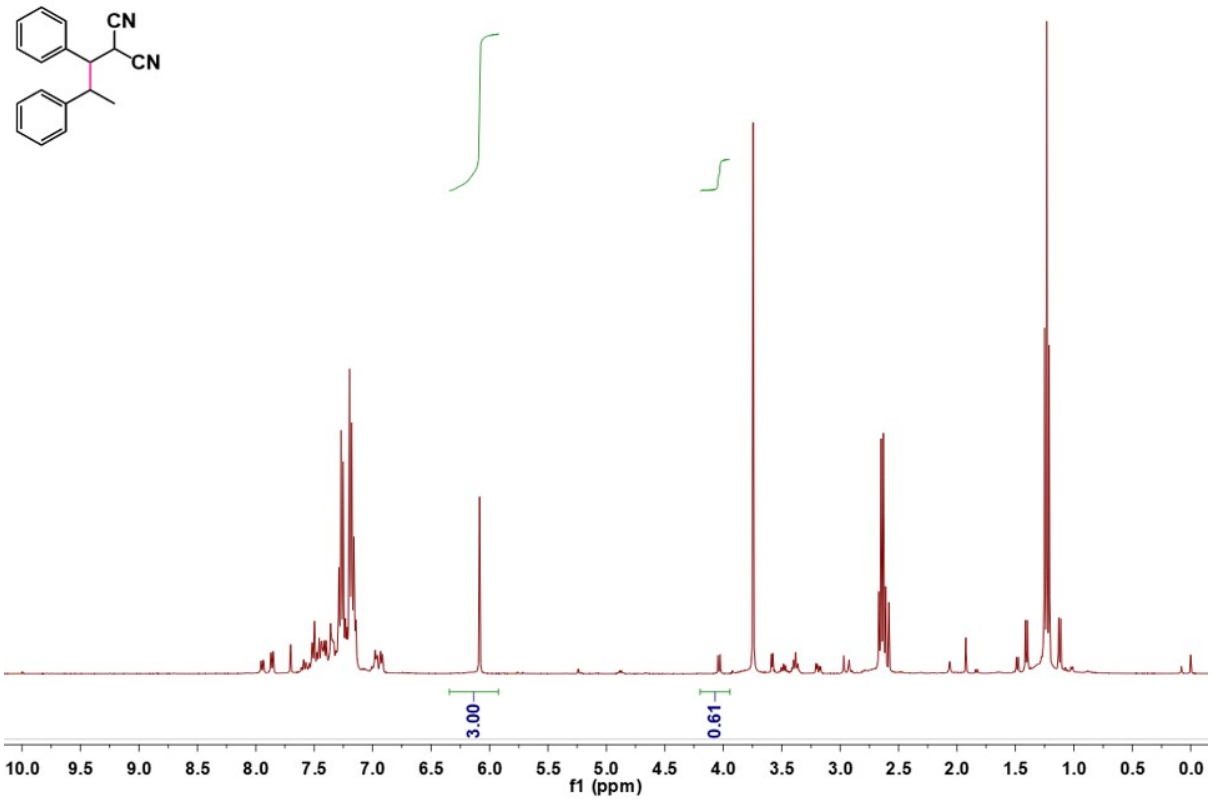

Figure S39. Crude ^{1}H NMR Spectrum for **5c**.

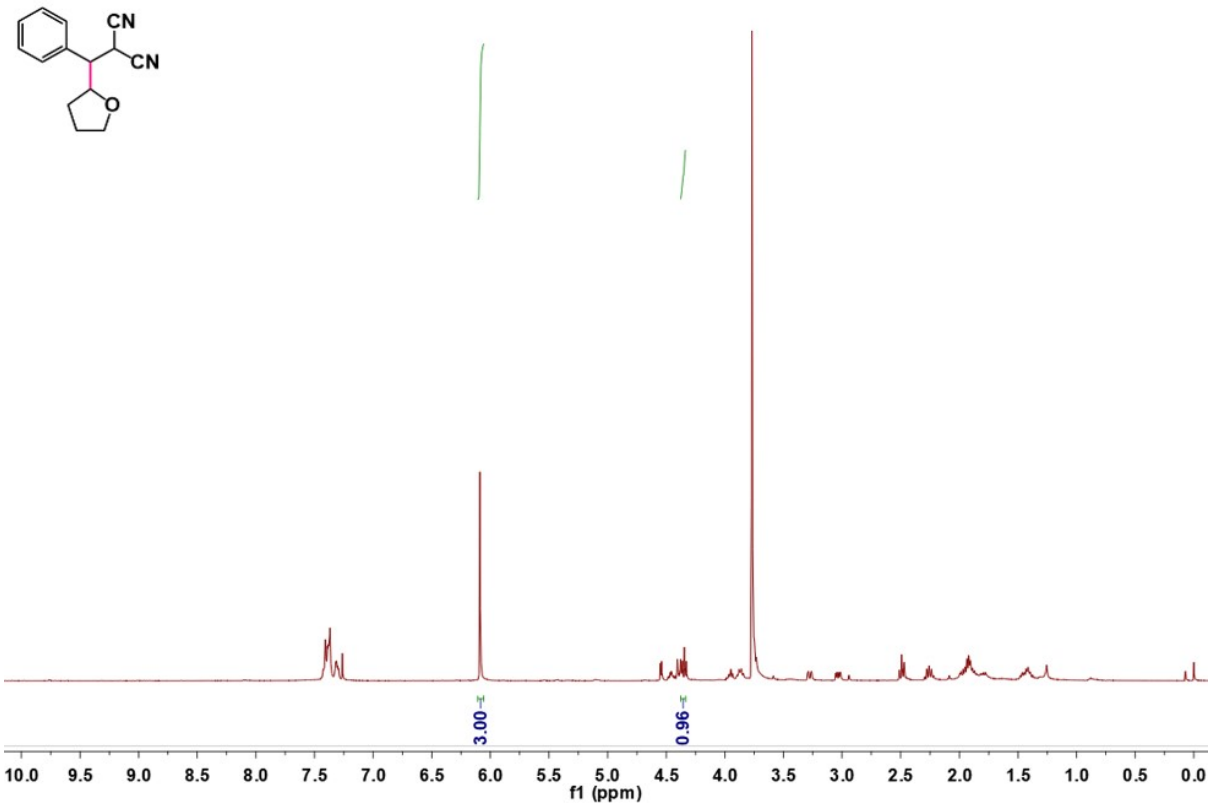

Figure S40. Crude ^{1}H NMR Spectrum for **6c**.

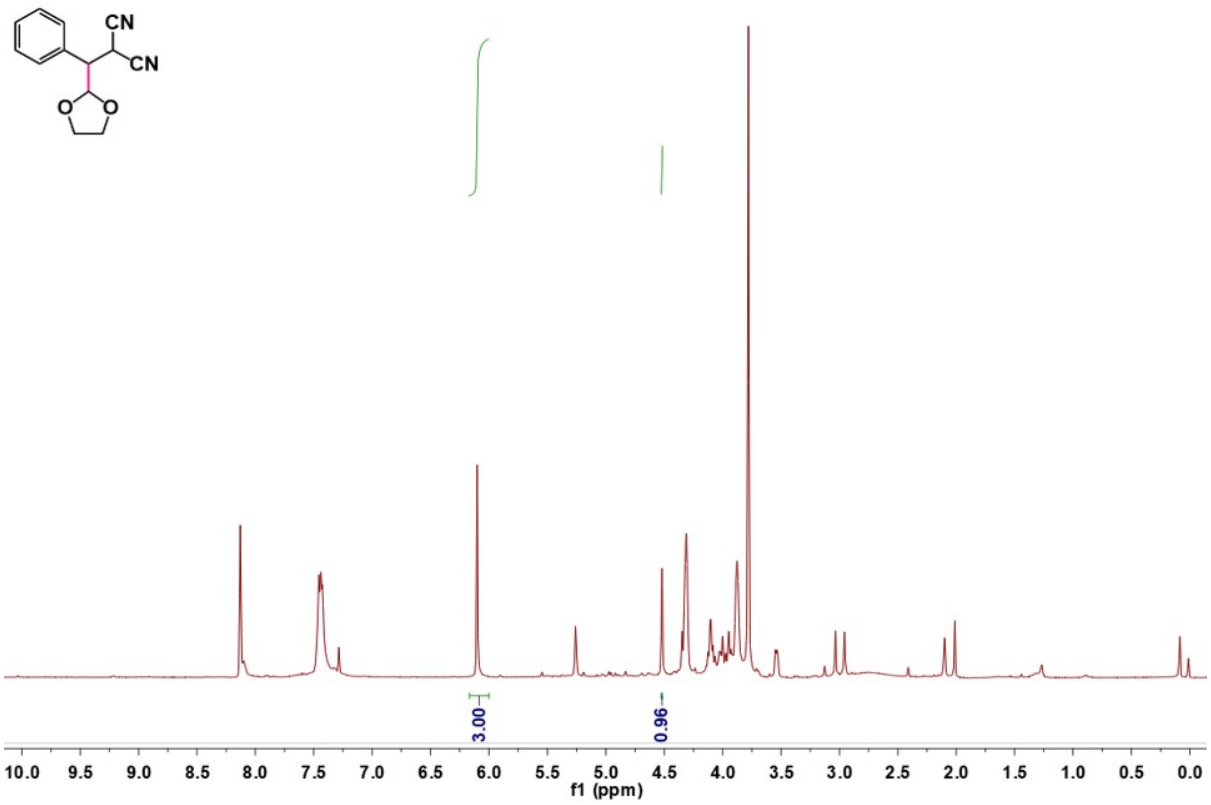

Figure S41. Crude ^{1}H NMR Spectrum for **7c**.

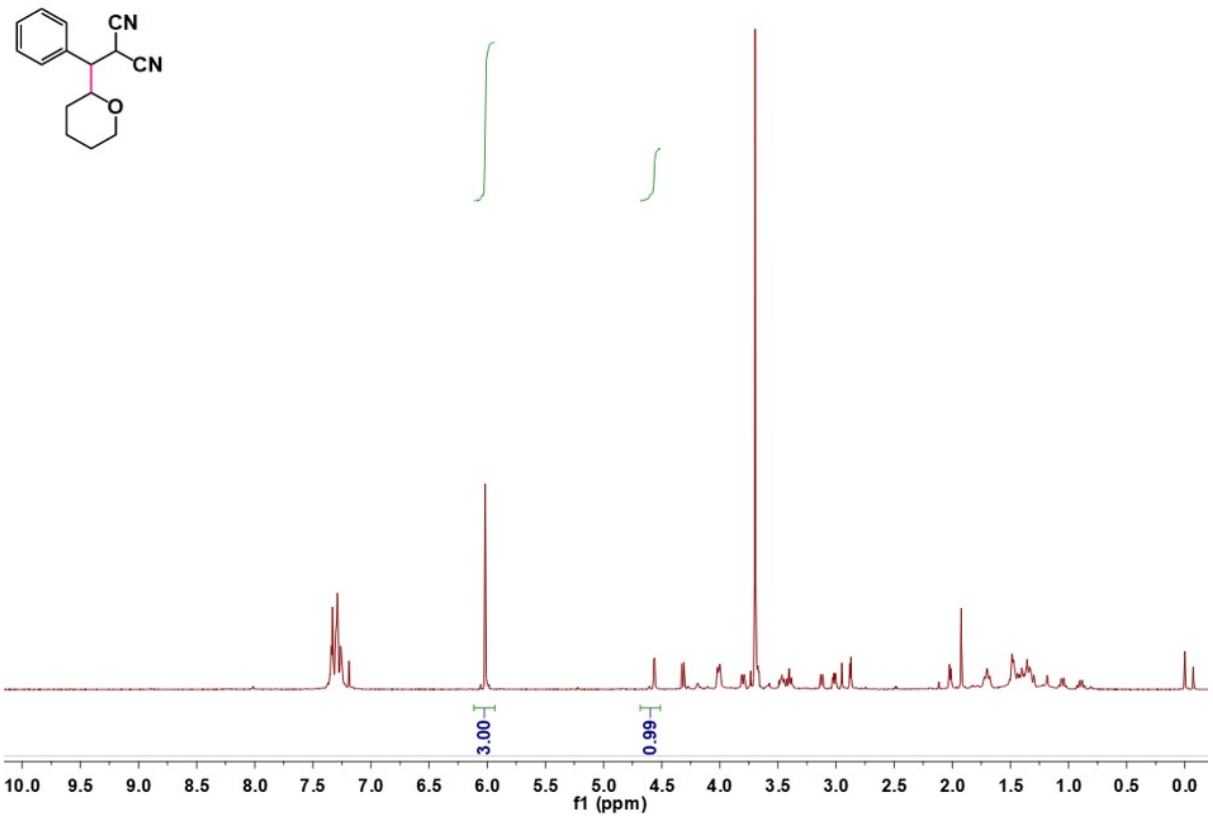

Figure S42. Crude ^{1}H NMR Spectrum for **8c**.

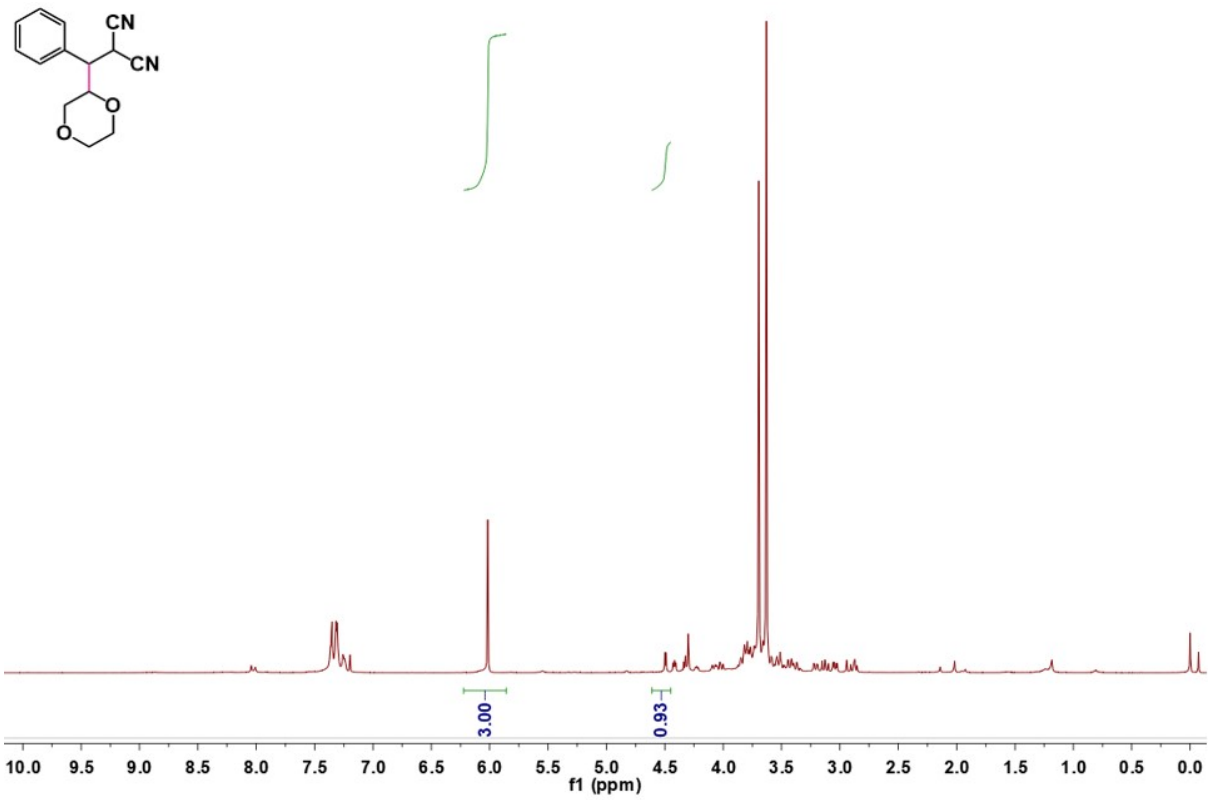

Figure S43. Crude ^{1}H NMR Spectrum for **9c**.

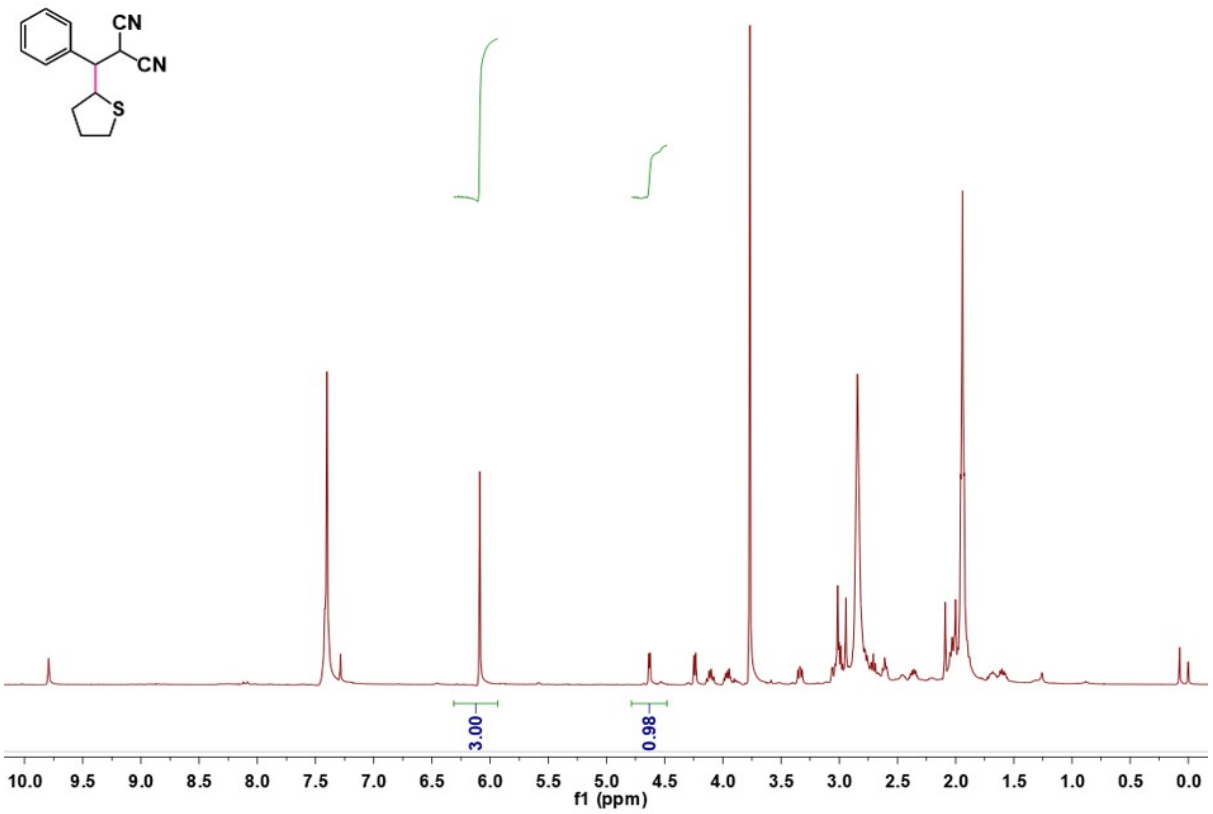

Figure S44. Crude ^{1}H NMR Spectrum for **10c**.

5. References

(1) Zhang, Z.; Yoshikawa, H.; Awaga, K. Monitoring the solid-state electrochemistry of Cu(2,7-AQDC) (AQDC = anthraquinone dicarboxylate) in a lithium battery: coexistence of metal and ligand redox activities in a metal–organic framework. *J. Am. Chem. Soc.*, **2014**, *136*, 16112−16115.

(2) Sun X., Luo X, Zhang X. Enhanced superoxide generation on defective surfaces for selective photooxidation. *J. Am. Chem. Soc.,* **2019**, *141*, 3797−3801.

(3) Zhao, L.; Du, Z.; Ji, G.; Wang, Y.; Cai, W.; He, C.; Duan, C. Eosin Y-Containing Metal−Organic Framework as a Heterogeneous Catalyst for Direct Photoactivation of Inert C−H Bonds. *Inorg. Chem.* **2022**, *61*, 7256−7265.